# Predicted charged charmoniumlike structures in the hidden-charm dipion decay of higher charmonia

Dian-Yong Chen[1,3] and Xiang Liu[1,2,*,†]

[1]*Research Center for Hadron and CSR Physics, Lanzhou University and Institute of Modern Physics of CAS, Lanzhou 730000, China*
[2]*School of Physical Science and Technology, Lanzhou University, Lanzhou 730000, China*
[3]*Nuclear Theory Group, Institute of Modern Physics of CAS, Lanzhou 730000, China*

(Received 1 July 2011; revised manuscript received 28 July 2011; published 19 August 2011)

In this work, we predict two charged charmoniumlike enhancement structures close to the $D^*\bar{D}$ and $D^*\bar{D}^*$ thresholds, where the Initial Single Pion Emission mechanism is introduced in the hidden-charm dipion decays of higher charmonia $\psi(4040)$, $\psi(4160)$, $\psi(4415)$ and charmoniumlike state $Y(4260)$. We suggest BESIII to search for these structures in the $J/\psi\pi^+$, $\psi(2S)\pi^+$ and $h_b(1P)\pi^+$ invariant mass spectra of the $\psi(4040)$ decays into $J/\psi\pi^+\pi^-$, $\psi(2S)\pi^+\pi^-$ and $h_b(1P)\pi^+\pi^-$. In addition, the experimental search for these enhancement structures in the $J/\psi\pi^+$, $\psi(2S)\pi^+$ and $h_c(1P)\pi^+$ invariant mass spectra of the $\psi(4260)$ hidden-charm dipion decays will be accessible at Belle and *BABAR*.

DOI: 10.1103/PhysRevD.84.034032 PACS numbers: 13.25.Gv, 13.75.Lb, 14.40.Pq

## I. INTRODUCTION

In past years, experimentalists have made big progress on the search for the charmoniumlike states, the so-called XYZ states, in the $B$ meson decay, the $e^+e^-$ collision, and the $\gamma\gamma$ fusion process, which has aroused extensive interest in revealing the underlying properties of the observed charmoniumlike states (see Refs. [1–5] for a review). The study of charmoniumlike states is a research field full of challenges and opportunities in hadron physics.

Very recently, the Belle Collaboration [6] reported two charged $Z_b$ structures around 10610 MeV and 10650 MeV by studying the $\Upsilon(nS)\pi^+$ $(n = 1, 2, 3)$ and $h_b(mP)\pi^+$ $(m = 1, 2)$ invariant mass spectra of $\Upsilon(5S) \to \Upsilon(nS)\pi^+\pi^-$, $h_b(mP)\pi^+\pi^-$ hidden-bottom decay channels (see Refs. [7–17] for theoretical progress). In Ref. [17], we proposed the initial single pion emission (ISPE) mechanism to explain the observed $Z_b$ structures. By emitting a pion, $\Upsilon(5S)$ decays into $B^{(*)}$ and $\bar{B}^{(*)}$ mesons with low momentum. Then, $B^{(*)}$ and $\bar{B}^{(*)}$ mesons interact with each other by exchanging $B^{(*)}$ meson and transit into $\Upsilon(nS)\pi^+$ or $h_b(mP)\pi^+$. Here, two structures near the $BB^*$ and $B^*B^*$ thresholds appear in the $\Upsilon(nS)\pi^+$ and $h_b(mP)\pi^+$ invariant mass spectra, which could correspond to $Z_b(10610)$ and $Z_b(10650)$ [6].

As just indicated in Ref. [17], if the ISPE mechanism is a universal mechanism existing in heavy quarkonium decay, we can naturally extend such a physical picture to study hidden-charm decays of higher vector charmonia due to the similarity between charmonium and bottomonium families, and predict some novel phenomena similar to the $Z_b$ structures.

In the Particle Data Book [18], six vector charmonia are established well, which are $J/\psi$, $\psi(2S)$, $\psi(3770)$, $\psi(4040)$, $\psi(4160)$, and $\psi(4415)$ with $I^G(J^{PC}) = 0^-(1^{--})$. Among these charmonia, only $\psi(4040)$, $\psi(4160)$, and $\psi(4415)$ are higher than the thresholds of $D\bar{D}$, $D\bar{D}^*$, and $D^*\bar{D}^*$. Thus, we study the hidden-charm decays of $\psi(4040)$, $\psi(4160)$ and $\psi(4415)$ via the ISPE mechanism. From the analysis of such modes, one indicates that enhancement structures similar to the charged $Z_b$ also exist in the charm case.

In addition, in this work we will study the hidden-charm decays of $Y(4260)$, which is an important charmoniumlike state observed by the *BABAR* Collaboration in the $e^+e^- \to \gamma_{ISR}J/\psi\pi^+\pi^-$ process [19]. Its mass, width, and $J^{PC}$ are $4263^{+8}_{-9}$ MeV, $95 \pm 14$ MeV,and $1^{--}$ [18]. The study presented in Ref. [20] indicates that $Y(4260)$ can be related to charmonia $\psi(4160)$ and $\psi(4415)$, where the $Y(4260)$ structure can be reproduced by the interference of production amplitudes of the $e^+e^- \to J/\psi\pi^+\pi^-$ processes via direct $e^+e^-$ annihilation and through intermediate charmonia $\psi(4160)$ and $\psi(4415)$ [20]. We naturally apply the ISPE mechanism existing in $\psi(4160)$ and $\psi(4415)$ decays to discuss the hidden-charm dipion decays of $Y(4260)$. Thus, studying $Y(4260)$ hidden-charm decays through the ISPE mechanism is an intriguing issue, where we will also predict some enhancement structure similar to the charged $Z_b$. As announced by *BABAR* [19], $Y(4260)$ was first observed in its $J/\psi\pi^+\pi^-$ decay channel. Searching enhancement structure in the $J/\psi\pi$ invariant mass spectrum of $Y(4260) \to J/\psi\pi^+\pi^-$ will be accessible in future experiments, which could provide a direct test to the nonresonant explanation for $Y(4260)$ proposed in [20].

This work is organized as follows. After the Introduction, we illustrate the hidden-charm dipion decays of higher charmonia under the ISPE mechanisms. In Sec. III, the numerical results are presented. The last section is the discussion and conclusion.

*Corresponding author
†xiangliu@lzu.edu.cn

 

## II. THE HIDDEN-CHARM DECAYS OF HIGHER CHARMONIA

### A. The ISPE mechanism

With $\psi(4040) \to J/\psi\pi^+\pi^-$ as an example, we first illustrate the possible decay mechanisms in the dipion hidden-charm decay of higher charmonium. $\psi(4040)$ can directly decay into $J/\psi\pi^+\pi^-$. In Refs. [21–23], the QCD Multipole Expansion method was proposed and can be applied to calculate such direct decay process. The second mechanism is that the dipion is from the intermediate scalar ($\sigma(600)$, $f_0(980)$) or tensor ($f_2(1270)$) meson, where the hadronic loops constructed by the $D^{(*)}$ mesons could be as a bridge to connect $\psi(4040)$ and $J/\psi\pi^+\pi^-$ (see Ref. [24] for more details).

The remaining decay mechanism existing in the hidden-charm dipion decays of higher charmonia is the ISPE mechanism, which was first proposed in Ref. [17]. By the quark-level diagram we give an explicit description (leftside diagram in Fig. 1) of the ISPE mechanism in $\psi(4040) \to J/\psi\pi^+\pi^-$ decay. The physical picture is that with a pion emission $\psi(4040)$ first dissolves into $D^{(*)}$ and $\bar{D}^{(*)}$ mesons with low momentum, which further turn into $J/\psi\pi^+$. Here, $D^{(*)}\bar{D}^{(*)} \to J/\psi\pi^+$ transition occurs via exchanging $D^{(*)}$ meson [17].

An equivalent hadron-level description is also presented in the rightside diagram of Fig. 1, which can be as an effective approach for dealing with the practical calculations.

### B. Effective Lagrangian and coupling constant

We adopt effective Lagrangian approach to calculate these hadron-level diagrams listed in Fig. 1. Here, the effective Lagrangians involved in the interaction vertexes in Fig. 1 include [25–27]

$$\begin{aligned}\mathcal{L}_{\psi' D^{(*)} D^{(*)}\pi} &= -ig_{\psi' DD\pi}\varepsilon^{\mu\nu\alpha\beta}\psi'_\mu\partial_\nu D\partial_\alpha\pi\partial_\beta\bar{D} \\ &+ g_{\psi' D^* D\pi}\psi'^\mu(D\pi\bar{D}^*_\mu + D^*_\mu\pi\bar{D}) \\ &- ig_{\psi' D^* D^*\pi}\varepsilon^{\mu\nu\alpha\beta}\psi'_\mu D^*_\nu\partial_\alpha\pi\bar{D}^*_\beta \\ &- ih_{\psi' D^* D^*\pi}\varepsilon^{\mu\nu\alpha\beta}\partial_\mu\psi'_\nu D^*_\alpha\pi\bar{D}^*_\beta,\end{aligned}$$

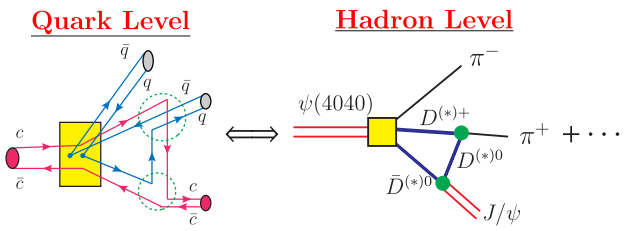


FIG. 1 (color online). (Color online.) The quark-level (leftside diagram) and hadron-level (right-side diagram) descriptions of the ISPE mechanism existing in the hidden-charm decays of higher charmonia.

where $\psi'$ denotes the initial state charmonium (one of the $\psi(4040)$, $\psi(4160)$, $\psi(4415)$ or $Y(4260)$). This Lagrangian reflects the initial state charmonium decays into $D^{(*)}\bar{D}^{(*)}\pi$.

$$\begin{aligned}\mathcal{L}_{D^* D^{(*)}\pi} &= ig_{D^* D\pi}(D^*_\mu\partial^\mu\pi\bar{D} - D\partial^\mu\pi\bar{D}^*_\mu) \\ &- g_{D^* D^*\pi}\varepsilon^{\mu\nu\alpha\beta}\partial_\mu D^*_\nu\pi\partial_\alpha\bar{D}^*_\beta, \\ \mathcal{L}_{\psi D^{(*)} D^{(*)}} &= ig_{\psi DD}\psi_\mu(\partial^\mu D\bar{D} - D\partial^\mu\bar{D}) \\ &- g_{\psi D^* D}\varepsilon^{\mu\nu\alpha\beta}\partial_\mu\psi_\nu(\partial_\alpha D^*_\beta\bar{D} + D\partial_\alpha\bar{D}^*_\beta) \\ &- ig_{\psi D^* D^*}\{\psi^\mu(\partial_\mu D^{*\nu}\bar{D}^*_\nu - D^{*\nu}\partial_\mu\bar{D}^*_\nu) \\ &+ (\partial_\mu\psi_\nu D^{*\nu} - \psi_\nu\partial_\mu D^{*\nu})\bar{D}^{*\mu} \\ &+ D^{*\mu}(\psi^\nu\partial_\mu\bar{D}^*_\nu - \partial_\mu\psi^\nu\bar{D}^*_\nu)\}, \\ \mathcal{L}_{h_c D^{(*)} D^{(*)}} &= g_{h_c D^* D}h_c^\mu(\bar{D}^*_\mu D + D^*_\mu\bar{D}) \\ &+ ig_{h_c D^* D^*}\varepsilon^{\mu\nu\alpha\beta}\partial_\mu h_{c\nu}D^*_\alpha\bar{D}^*_\beta,\end{aligned}$$

which will be applied to describe a rescattering mechanism involving in the two charmed mesons into $J/\psi\pi$ or $h_c\pi$ by exchanging a $D^{(*)}$ meson. In the above Lagrangians, $D$ and $D^*$ are grouped together on the basis of heavy quark symmetry while that pions appear as the result of a representation of the chiral symmetry. In addition, we define charm meson isodoublets as $D^{(*)} = (D^{(*)0}, D^{(*)+})$, $\bar{D}^{(*)T} = (\bar{D}^{(*)0}, D^{(*)-})$, and $\pi = \boldsymbol{\tau}\cdot\boldsymbol{\pi}$ [25].

The values of the coupling constants can be determined by the relations

$$\begin{aligned}g_{\psi DD} &= g_{\psi D^* D^*}\frac{m_D}{m^*_D} = g_{\psi D^* D}m_\psi\sqrt{\frac{m_D}{m^*_D}} = \frac{m_\psi}{f_\psi}, \\ g_{h_c DD^*} &= -2g_1\sqrt{m_{h_c}m_D m_{D^*}}, \\ g_{h_c D^* D^*} &= 2g_1\frac{m_{D^*}}{\sqrt{m_{h_c}}}, \\ g_{D^* D^*\pi} &= \frac{g_{D^* D\pi}}{\sqrt{m_D m_{D^*}}} = \frac{2g}{f_\pi}, \\ g_1 &= -\sqrt{\frac{m_{\chi_{c0}}}{3}}\frac{1}{f_{\chi_{c0}}},\end{aligned}$$

where $f_\psi = 0.416$ GeV and $f_{\chi_{c0}} = 0.297$ GeV are the decay constants of $\psi$ and $\chi_{c0}$, respectively. In addition, $f_{\chi_{c0}} \simeq 0.51$ GeV can be approximately determined by the QCD sum rule approach [27]. With the measured branching ratio of $D^* \to D\pi$ by CLEO-c [28] and $f_\pi = 132$ MeV, one gets $g = 0.59$ [29].

### C. Decay Amplitudes

With these Lagrangians just listed above, we write out the decay amplitude for the dipion transition between $\psi(4040)$ and $J/\psi$, i.e., there are three interaction vertexes and three $D^{(*)}$ propagators, which are obtained by the effective Lagrangian presented in Sec. IIb. Additionally, we also introduce the monopole form factor $\mathcal{F}(q^2)$ in

decay amplitudes, which is taken as $\mathcal{F}(q^2) = (\Lambda^2 - m_E^2)/(q^2 - m_E^2)$. Here, $m_E$ is the mass of the exchanged meson while the phenomenological parameter $\Lambda$ can be parameterized as $\Lambda = m_E + \beta\Lambda_{\rm QCD}$ with $\Lambda_{\rm QCD} = 220$ MeV. Such monopole form factor is introduced to describe the structure effects of the interaction vertices as well as the off-shell effects of the exchanged charmed mesons for $D^{(*)}\bar{D}^{(*)} \to J/\psi\pi^{\pm}, h_c(1P)\pi^{\pm}$ transitions in $\psi(4040) \to J/\psi\pi^+\pi^-, h_c(1P)\pi^+\pi^-$ decays.

When only considering the intermediate $D^*\bar{D}$ + H.c. contributions to $\psi(4040) \to J/\psi\pi^+\pi^-$, there are 12 diagrams just shown in Fig. 2. Among these diagrams, there are only six independent diagrams if considering $SU(2)$ symmetry, i.e., Fig. 2 (i) can be transferred into Fig. 2 $(i+6)$ $(i = 1, \cdots, 6)$ by transformations $D^{(*)+} \rightleftharpoons \bar{D}^{(*)0}$ and $D^{(*)-} \rightleftharpoons D^{(*)0}$. Thus, the total decay amplitude for $\psi(4040) \to J/\psi(p_5)\pi^+(p_3)\pi^-(p_4)$ with the intermediate $D^*(p_1)\bar{D}(p_2) + D(p_1)\bar{D}^*(p_2)$ contributions are expressed as

$$\mathcal{M}[\psi(4040) \to J/\psi\pi^+\pi^-]_{D^*\bar{D}+\text{H.c.}} = 2\sum_{i=1,\cdots,6} M^{(i)}_{D^*\bar{D}+\text{H.c.}}, \quad (1)$$

where we mark the four momenta of the corresponding mesons. Factor 2 reflects $SU(2)$ symmetry mentioned above. The subscript $D^*\bar{D}$ + H.c. denotes that $\psi(4040) \to J/\psi\pi^+\pi^-$ occurs via the intermediate $D^*\bar{D} + D\bar{D}^*$. The expressions of decay amplitudes $M^{(i)}_{D^*\bar{D}+\text{H.c.}}$ $(i = 1, 2, 3)$ read as

$$\begin{aligned} M^{(1)}_{D^*\bar{D}+\text{H.c.}} &= (i)^3 \int \frac{d^4q}{(2\pi)^4}[g_{\psi' D^* D\pi}\epsilon^{\mu}_{\psi}][ig_{D^*D^*\pi}(iP_4^{\rho})] \\ &\times [-ig_{J/\psi D^* D^*}\epsilon^{\nu}_{J/\psi}((-iq_{\nu} + ip_{2\nu})g_{\theta\phi} \\ &+ (iP_{5\phi} + iq_{\phi})g_{\nu\theta} - (ip_{2\theta}ip_{5\theta})g_{\nu\phi})] \\ &\times \frac{1}{p_1^2 - m_D^2}\frac{-g_{\mu}^{\phi} + p_{1\mu}p_1^{\phi}/m_{D^*}^2}{p_2^2 - m_{D^*}^2} \\ &\times \frac{-g_{\rho}^{\theta} + q_{\rho}q^{\theta}/m_{D^*}^2}{q^2 - m_{D^*}^2}\mathcal{F}^2(q^2), \end{aligned} \quad (2)$$

$$\begin{aligned} M^{(2)}_{D^*\bar{D}+\text{H.c.}} &= (i)^3 \int \frac{d^4q}{(2\pi)^4}[g_{\psi' D^* D\pi}\epsilon^{\mu}_{\psi}][ig_{D^*D\pi}(-ip_4^{\rho})] \\ &\times [ig_{J/\psi DD}\epsilon^{\nu}_{J/\psi}(ip_{2\nu} - iq_{\nu})] \\ &\times \frac{-g_{\mu\rho} + p_{1\mu}p_{1\rho}/m_{D^*}^2}{p_1^2 - m_{D^*}^2}\frac{1}{p_2^2 - m_D^2} \\ &\times \frac{1}{q^2 - m_D^2}\mathcal{F}^2(q^2), \end{aligned} \quad (3)$$

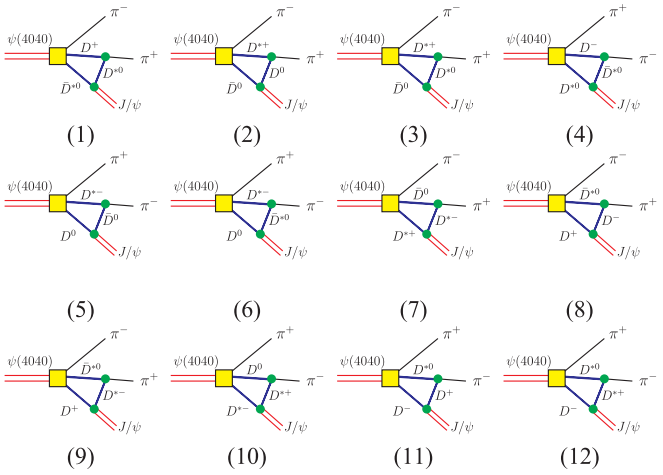


FIG. 2 (color online). (Color online.) The hadron-level diagrams for $\psi(4040) \to J/\psi\pi^+\pi^-$ decays with $D^*\bar{D}$ + H.c as the intermediate states.

$$\begin{aligned} M^{(3)}_{D^*\bar{D}+\text{H.c.}} &= (i)^3 \int \frac{d^4q}{(2\pi)^4}[g_{\psi' D^* D\pi}\epsilon^{\mu}_{\psi}] \\ &\times [-g_{D^*D^*\pi}\varepsilon^{\theta\phi\delta\tau}(iq^{\theta})(-ip_1^{\delta})] \\ &\times [-g_{J/\psi D^* D}\varepsilon^{\rho\nu\alpha\beta}(ip_{5\rho})\epsilon_{J/\psi\nu}(-iq_{\alpha})] \\ &\times \frac{-g_{\mu\tau} + p_{1\mu}p_{1\tau}/m_{D^*}^2}{p_1^2 - m_{D^*}^2}\frac{1}{p_2^2 - m_D^2} \\ &\times \frac{-g_{\beta\phi} + q_{\beta}q_{\phi}/m_{D^*}^2}{q^2 - m_{D^*}^2}\mathcal{F}^2(q^2), \end{aligned} \quad (4)$$

which correspond to the dipion transitions between $\psi(4040)$ and $J/\psi$ with a initial single pion $(\pi^-)$ emission. $M^{(4)}_{D^*\bar{D}+\text{H.c.}}$, $M^{(5)}_{D^*\bar{D}+\text{H.c.}}$ and $M^{(6)}_{D^*\bar{D}+\text{H.c.}}$ can be obtained by $M^{(1)}_{D^*\bar{D}+\text{H.c.}}$, $M^{(2)}_{D^*\bar{D}+\text{H.c.}}$ and $M^{(3)}_{D^*\bar{D}+\text{H.c.}}$ respectively if making the replacement $p_3 \rightleftharpoons p_4$ in Eqs. (2)–(4). Here, $M^{(j)}_{D^*\bar{D}+\text{H.c.}}$ $(j = 4, 5, 6)$ are decay amplitudes of the dipion transitions between $\psi(4040)$ and $J/\psi$ with a initial single pion $(\pi^+)$ emission.

We also present the decay amplitude of $\psi(4040) \to J/\psi(p_5)\pi^+(p_3)\pi^-(p_4)$ via the intermediate $D^*(p_1)\bar{D}^*(p_2)$.

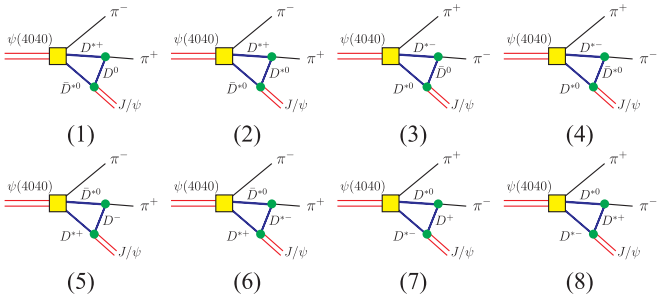


FIG. 3 (color online). (Color online.) The hadron-level diagrams for $\psi(4040) \to J/\psi\pi^+\pi^-$ decays with $D^*\bar{D}^*$ as the intermediate states.

$$\mathcal{M}[\psi(4040)\to J/\psi\pi^+\pi^-]_{D^*\bar{D}^*}=2\sum_{\alpha=1,\cdots,4}M^{(\alpha)}_{D^*\bar{D}^*}. \quad (5)$$

We list all diagrams contributing to $\psi(4040)\to J/\psi\pi^+\pi^-$ in Fig. 3. Among these eight eight diagrams, Fig. 2 $(\alpha)$ can be obtained by Fig. 2 $(\alpha+4)$ $(\alpha=1,\cdots,4)$ if making the transformations $D^{(*)+}\rightleftharpoons\bar{D}^{(*)0}$ and $D^{(*)-}\rightleftharpoons D^{(*)0}$, which results in factor 2 in Eq. (5) due to $SU(2)$ symmetry.

The decay amplitudes $M^{(1)}_{D^*\bar{D}^*}$ and $M^{(2)}_{D^*\bar{D}^*}$ are expressed as

$$M^{(1)}_{D^*\bar{D}^*}=(i)^3\int\frac{d^4q}{(2\pi)^4}[-ig_{\psi' D^*D^*\pi}\varepsilon^{\mu\rho\alpha\beta}\epsilon_{\psi\mu}(ip_{3\alpha})-ih_{\psi' D^*D^*\pi}\varepsilon^{\alpha\mu\rho\beta}\epsilon_{\psi\mu}(-ip_{0\alpha})][ig_{D^*D\pi}(-ip_{4\lambda})]$$
$$\times[-g_{J/\psi D^*D}\varepsilon_{\delta\nu\theta\phi}(ip_5^\delta)\epsilon^\nu_{J/\psi}(-ip_2^\theta)]\frac{-g_\rho^\lambda+p_{1\rho}p_1^\lambda/m^2_{D^*}}{p_1^2-m^2_{D^*}}\frac{-g_\beta^\phi+p_{2\beta}p_2^\phi/m^2_{D^*}}{p_2^2-m^2_{D^*}}\frac{1}{q^2-m_D^2}\mathcal{F}^2(q^2), \quad (6)$$

$$M^{(2)}_{D^*\bar{D}^*}=(i)^3\int\frac{d^4q}{(2\pi)^4}[-ig_{\psi' D^*D^*\pi}\varepsilon^{\mu\rho\alpha\beta}\epsilon_{\psi\mu}(ip_{3\alpha})-ih_{\psi' D^*D^*\pi}\varepsilon^{\alpha\mu\rho\beta}\epsilon_{\psi\mu}(-ip_{0\alpha})][-g_{D^*D^*\pi}\varepsilon^{\delta\tau\theta\phi}(-ip_{1\delta})(iq_\theta)]$$
$$\times[-ig_{J/\psi D^*D^*}\epsilon^\nu_{J/\psi}((-iq_\nu+ip_{2\nu}))g_{\omega\lambda}+(ip_{5\omega}+iq_\omega)g_{\nu\lambda}$$
$$+(-ip_{2\lambda}-ip_{5\lambda})g_{\nu\omega}]\frac{-g^{\rho\tau}+p_{1\rho}p_{1\tau}/m^2_{D^*}}{p_1^2-m^2_{D^*}}\frac{-g_\beta^\omega+p_{2\beta}p_2^\omega/m^2_{D^*}}{p_2^2-m^2_{D^*}}\frac{-g_\phi^\lambda+q_\phi q^\lambda/m^2_{D^*}}{q^2-m^2_{D^*}}\mathcal{F}^2(q^2). \quad (7)$$

Thus, by Eqs. (6) and (7), we can easily obtain decay amplitudes $M^{(3)}_{D^*\bar{D}^*}$ and $M^{(4)}_{D^*\bar{D}^*}$ corresponding to Fig. 3(c) and 3(d) where the transformation $p_3\rightleftharpoons p_4$ is performed.

In the following, we extend the same framework to study the dipion transition between $\psi(4040)$ and $h_c(1P)$. By replacing $J/\psi$ with $h_c(1P)$ in Figs. 2(a), 2(c), 2(d), 2(f), 2(g), 2(i), 2(j), 2(l), and 3, we obtain all diagrams relevant to $\psi(4040)\to h_c(1P)\pi^+\pi^-$ decay. The total decay amplitudes of $\psi(4040)\to h_c(1P)(p_5)\pi^+(p_3)\pi^-(p_4)$ via $D^*(p_1)\bar{D}(p_2)+D(p_1)\bar{D}^*(p_2)$ and $D^*(p_1)\bar{D}^*(p_2)$ are

$$\mathcal{M}[\psi(4040)\to h_c(1P)\pi^+\pi^-]_{D^*\bar{D}+\text{H.c.}}=2\sum_{\beta=1,\cdots,4}A^{(\beta)}_{D^*\bar{D}+\text{H.c.}}, \quad (8)$$

$$\mathcal{M}[\psi(4040)\to h_c(1P)\pi^+\pi^-]_{D^*\bar{D}^*}=2\sum_{\kappa=1,\cdots,4}A^{(\kappa)}_{D^*\bar{D}^*}, \quad (9)$$

respectively, where the concrete amplitude expressions are

$$A^{(1)}_{D^*\bar{D}+\text{H.c.}}=(i)^3\int\frac{d^4q}{(2\pi)^4}[g_{\psi' D^*D^*\pi}\epsilon^\mu_\psi][ig_{D^*D\pi}(-ip_4^\rho)][ig_{h_cD^*D^*}\varepsilon_{\delta\nu\theta\phi}(ip_5^\delta)\epsilon^\nu_{h_c}]\frac{1}{p_1^2-m_D^2}\frac{-g_\mu^\phi+p_{2\mu}p_2^\phi/m^2_{D^*}}{p_2^2-m^2_{D^*}}$$
$$\times\frac{-g_\rho^\theta+q_\rho q^\theta/m^2_{D^*}}{q^2-m^2_{D^*}}\mathcal{F}^2(q^2), \quad (10)$$

$$A^{(2)}_{D^*\bar{D}+\text{H.c.}}=(i)^3\int\frac{d^4q}{(2\pi)^4}[g_{\psi' D^*D^*\pi}\epsilon^\mu_\psi][-g_{D^*D^*\pi}\varepsilon_{\theta\phi\delta\tau}(iq^\theta)(-ip_1^\delta)][g_{h_cD^*D}\epsilon_{h_c\nu}]\frac{-g_\mu^\phi+p_{1\mu}p_1^\phi/m^2_{D^*}}{p_1^2-m^2_{D^*}}\frac{1}{p_2^2-m_D^2}$$
$$\times\frac{-g^{\nu\tau}+q^\nu q^\tau/m^2_{D^*}}{q^2-m^2_{D^*}}\mathcal{F}^2(q^2), \quad (11)$$

and

$$A^{(1)}_{D^*\bar{D}^*}=(i)^3\int\frac{d^4q}{(2\pi)^4}[-ig_{\psi' D^*D^*\pi}\varepsilon_{\mu\rho\alpha\beta}\epsilon^\mu_\psi(ip_3^\alpha-ip_0^\alpha)][ig_{D^*D\pi}(-ip_{4\lambda})][g_{h_cD^*D}\epsilon_{h_c\nu}]\frac{-g^{\rho\lambda}+p_1^\rho p_1^\lambda/m^2_{D^*}}{p_1^2-m^2_{D^*}}$$
$$\times\frac{-g^{\beta\nu}+p_2^\beta p_2^\nu/m^2_{D^*}}{p_2^2-m^2_{D^*}}\frac{1}{q^2-m_D^2}\mathcal{F}^2(q^2), \quad (12)$$

$$A^{(2)}_{D^*\bar{D}^*} = (i)^3 \int \frac{d^4q}{(2\pi)^4}[-ig_{\psi' D^* D^* \pi}\varepsilon_{\mu\rho\alpha\beta}\epsilon^{\mu}_{\psi}(ip_3^{\alpha} - ip_0^{\alpha})][-g_{D^* D^* \pi}\epsilon_{\delta\tau\theta\phi}(-ip_1^{\delta})(iq^{\theta})][ig_{h_c D^* D^*}\varepsilon_{\kappa\nu\lambda\omega}(ip_5^{\kappa})\epsilon^{\nu}_{h_c}] \times \frac{-g^{\rho\tau} + p_1^{\rho}p_1^{\tau}/m^2_{D^*}}{p_1^2 - m^2_{D^*}} \frac{-g^{\beta\omega} + p_2^{\beta}p_2^{\omega}/m^2_{D^*}}{p_2^2 - m^2_{D^*}} \frac{-g^{\phi\lambda} + q^{\phi}q^{\lambda}/m^2_{D^*}}{q^2 - m^2_{D^*}} \mathcal{F}^2(q^2). \quad (13)$$

After performing the transformation $p_3 \rightleftharpoons p_4$, $A^{(1)}_{D^*\bar{D}+\text{H.c.}}$, $A^{(2)}_{D^*\bar{D}+\text{H.c.}}$, $A^{(1)}_{D^*\bar{D}^*}$, and $A^{(2)}_{D^*\bar{D}^*}$ can be transferred into $A^{(3)}_{D^*\bar{D}+\text{H.c.}}$, $A^{(4)}_{D^*\bar{D}+\text{H.c.}}$, $A^{(3)}_{D^*\bar{D}^*}$, and $A^{(4)}_{D^*\bar{D}^*}$, respectively.

The differential decay width for $\psi(4040) \to J/\psi\pi^+\pi^-$ reads as

$$d\Gamma = \frac{1}{3}\frac{1}{(2\pi)^3}\frac{1}{32m^3_{\psi(4040)}}\overline{|\mathcal{M}^2|}dm^2_{J/\psi\pi^+}dm^2_{\pi^+\pi^-} \quad (14)$$

with $m^2_{J/\psi\pi^+} = (p_4 + p_5)^2$ and $m^2_{\pi^+\pi^-} = (p_3 + p_4)^2$, where the overline indicates the average over the polarizations of the $\psi(4040)$ in the initial state and the sum over the polarization of $J/\psi(4040)$ in the final state. Replacing $m_{J/\psi\pi^+}$ with $m_{\psi(2S)\pi^+}$ or $m_{h_c(1P)\pi^+}$, we obtain the differential decay width for $\psi(4040) \to \psi(2S)\pi^+\pi^-$ or $\psi(4040) \to h_c(1P)\pi^+\pi^-$.

When studying the hidden-charm dipion decay of other higher charmonia $\psi(4160)$, $\psi(4415)$ and charmoniumlike state $Y(4260)$, we only need to replace the relevant coupling constants and the masses in the formulism of the $\psi(4040)$ decays.

## III. NUMERICAL RESULT

In this work, we are mainly concerned with the line shapes of the differential decay widths of $\psi(4040)$, $\psi(4160)$, $\psi(4415)$, and charmoniumlike state $Y(4260)$ decays into $J/\psi\pi^+\pi^-$, $\psi(2S)\pi^+\pi^-$ and $h_c(1P)\pi^+\pi^-$, which are dependent on the invariant mass spectra of $J/\psi\pi^+$, $\psi(2S)\pi^+$, and $h_c(1P)\pi^+$. Thus, we set the coupling constants of $\psi D^{(*)}\bar{D}^{(*)}\pi$ as 1 in our calculation. Besides these coupling constants listed in Sec. IIb, other input parameters are the masses involved in our calculation, which are taken from Particle Data Book [18].

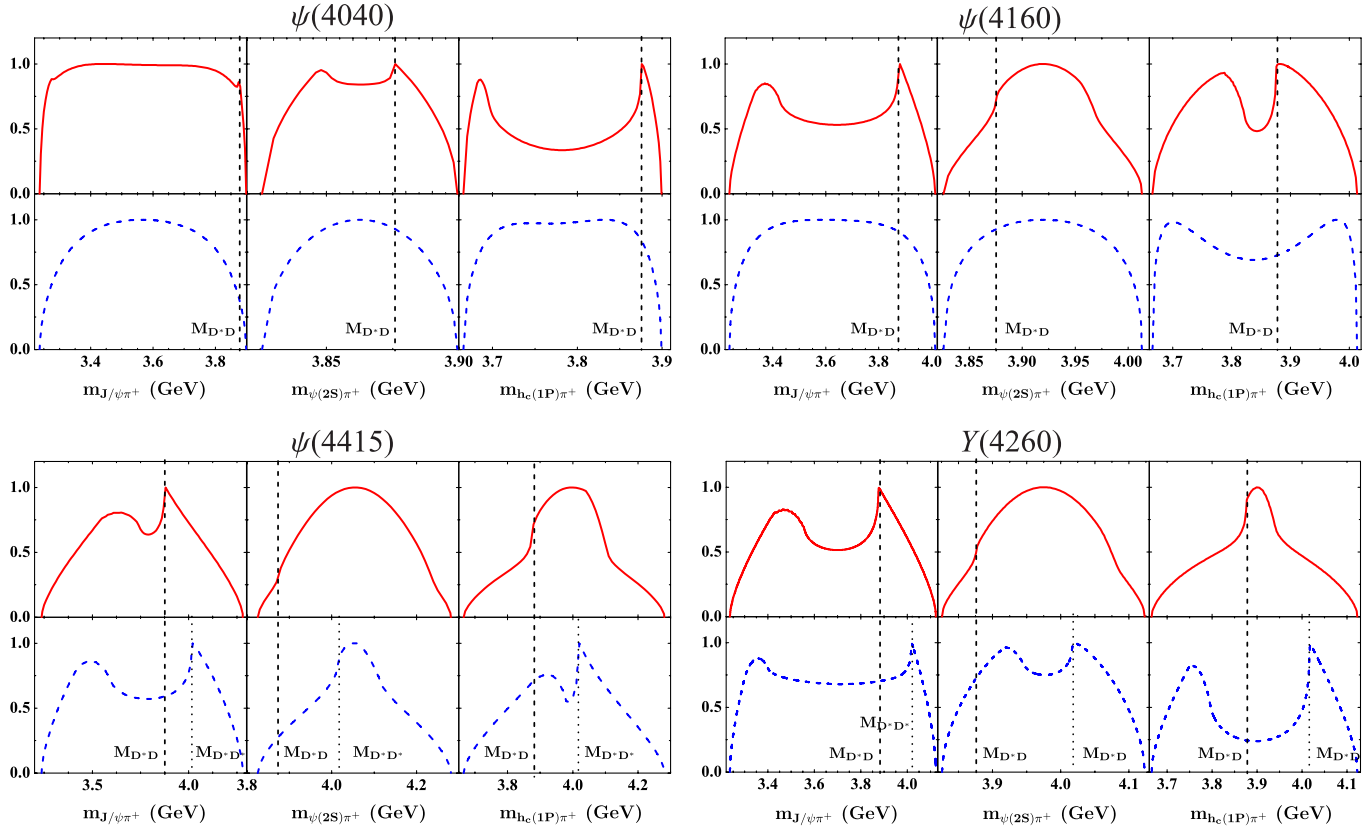


FIG. 4 (color online). (Color online.) The invariant mass spectra of $J/\psi\pi^+$, $\psi(2S)\pi^+$, and $h_c(1P)\pi^+$ for the $\psi(4040)$, $\psi(4160)$, $\psi(4415)$, and $Y(4260)$ decays into $J/\psi\pi^+\pi^-$, $\psi(2S)\pi^+\pi^-$, and $h_c(1P)\pi^+\pi^-$. Here, the solid, dashed correspond to the results considering intermediate $D\bar{D}^*$ + H.c. and $D^*\bar{D}^*$, respectively, in Fig. 1. The vertical dashed lines and the dotted lines denote the threshold of $D^*\bar{D}$ and $D^*\bar{D}^*$, respectively. Here, the maximum of the line shape is normalized to 1.

In Fig. 4, we present the results of $d\Gamma/dm_{J/\psi\pi^+}$, $d\Gamma/dm_{\psi(2S)\pi^+}$, and $d\Gamma/dm_{h_c(1P)\pi^+}$ of $\psi(4040)$, $\psi(4160)$, $\psi(4415)$, $Y(4260)$ decays into $J/\psi\pi^+\pi^-$, $\psi(2S)\pi^+\pi^-$, $h_c(1P)\pi^+\pi^-$.

(1) There exit sharp peak structures close to the $D^*\bar{D}$ threshold and the corresponding reflections in the distributions of $d\Gamma/dm_{J/\psi\pi^+}$, $d\Gamma/dm_{\psi(2S)\pi^+}$ and $d\Gamma/dm_{h_c(1P)\pi^+}$ of $\psi(4040) \to J/\psi\pi^+\pi^-$, $\psi(4040) \to \psi(2S)\pi^+\pi^-$, and $\psi(4040) \to h_c(1P)\pi^+\pi^-$ decays. We notice that this structure appearing in $d\Gamma(\psi(4040) \to J/\psi\pi^+\pi^-)/dm_{J/\psi\pi^+}$ is not obvious when compared to the structure in $d\Gamma(\psi(4040) \to \psi(2S)\pi^+\pi^-)/dm_{\psi(2S)\pi^+}$ or $d\Gamma(\psi(4040) \to h_c(1P)\pi^+\pi^-)/dm_{h_c(1P)\pi^+}$ distribution.

(2) Two sharp peaks appear in the $d\Gamma(\psi(4160) \to J/\psi\pi^+\pi^-)/dm_{J/\psi\pi^+}$ and $d\Gamma(\psi(4160) \to h_c(1P)\pi^+\pi^-)/dm_{h_c(1P)\pi^+}$ distributions, which are close to the $D^*\bar{D}$ threshold. The structure in the $J/\psi\pi^+$ invariant mass spectrum is more narrow than that in the $h_c(1P)\pi^+$ invariant mass spectrum.

(3) In the hidden-charm dipion decays of $\psi(4415)$, we find two sharp peak structures around the $D^*\bar{D}$ and $D^*\bar{D}^*$ thresholds appearing in the $J/\psi\pi^+$ invariant mass spectra. In addition, a sharp peak close the $D^*\bar{D}^*$ threshold is observed in the $h_c(1P)\pi^+$ invariant mass spectrum distribution. In the $d\Gamma(\psi(4415) \to \psi(2S)\pi^+\pi^-)/dm_{\psi(2S)\pi^+}$ distribution, a peak near $D^*\bar{D}^*$ with its reflection form a broad structure. Under the ISPE mechanism, the intermediate $D^*\bar{D}$ can result in a very broad structure in the $h_c(1P)\pi^+$ invariant mass spectrum distribution.

(4) There exist the sharp peaks close to the $D^*\bar{D}$ threshold in the $d\Gamma(\psi(4260) \to J/\psi\pi^+\pi^-)/dm_{J/\psi\pi^+}$ and $d\Gamma(\psi(4260) \to h_c(1P)\pi^+\pi^-)/dm_{h_c(1P)\pi^+}$ distributions, the structures around $D^*\bar{D}^*$ threshold in the $d\Gamma(\psi(4260) \to \psi(2S)\pi^+\pi^-)/dm_{\psi(2S)\pi^+}$, and $d\Gamma(\psi(4260) \to h_c(1P)\pi^+\pi^-)/dm_{h_c(1P)\pi^+}$ distributions. The peak closes the $D^*\bar{D}$ threshold and its reflection overlap with each to form a broad structure in the $h_c\pi^+$ invariant mass spectrum.

We need to specify that the result presented in Fig. 4 is obtained by taking $\beta = 1$. Our study shows that the line shapes in Fig. 4 are weakly dependent on the values of $\beta$. With $\psi(4415) \to h_c\pi^+\pi^-$ as an example, in Fig. 5 we illustrate the $\beta$ dependence of $d\Gamma(\psi(4415) \to h_c(1P)\pi^+\pi^-)/dm_{h_c(1P)\pi^+}$ distribution, where the line shapes corresponding to $\beta = 1, 2, 3$ remain almost unchanged.

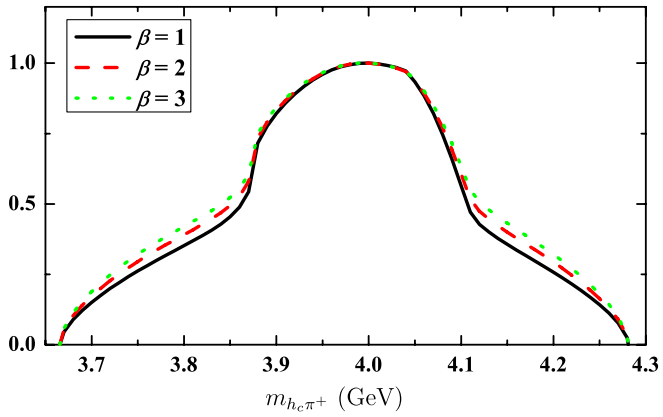


FIG. 5 (color online). (Color online.) The dependence of $d\Gamma(\psi(4415) \to h_c(1P)\pi^+\pi^-)/dm_{h_c(1P)\pi^+}$ distribution on $\beta$. Here, $\psi(4415) \to h_c(1P)\pi^+\pi^-$ occurs via the intermediate $D^*\bar{D}$ + H.c.

## IV. DISCUSSION AND CONCLUSION

In this work, we study the line shapes of the differential decay widths of $\psi(4040)$, $\psi(4160)$, $\psi(4415)$ and charmoniumlike state $Y(4260)$ decays into $J/\psi\pi^+\pi^-$, $\psi(2S)\pi^+\pi^-$ and $h_c(1P)\pi^+\pi^-$, where the ISPE mechanism is introduced. Furthermore, we predict the sharp peak structures close to $D^*\bar{D}$ and $D^*\bar{D}^*$ thresholds appearing the corresponding $J/\psi\pi^+$, $\psi(2S)\pi^+$ and $h_c(1P)\pi^+$ invariant mass spectra.

The ISPE mechanism plays a crucial role to form these novel charged charmoniumlike structures in the hidden-charm dipion decays of higher charmonia. To some extent, these predicted structures are the charmonium analogue of two newly observed $Z_b$ structures in the hidden-bottom dipion decays of $\Upsilon(5S)$ [6].

We suggest further experimental search for these predicted charmoniumlike structures close to the $D^*\bar{D}$ and $D^*\bar{D}^*$ thresholds. Recently, BESIII has stated

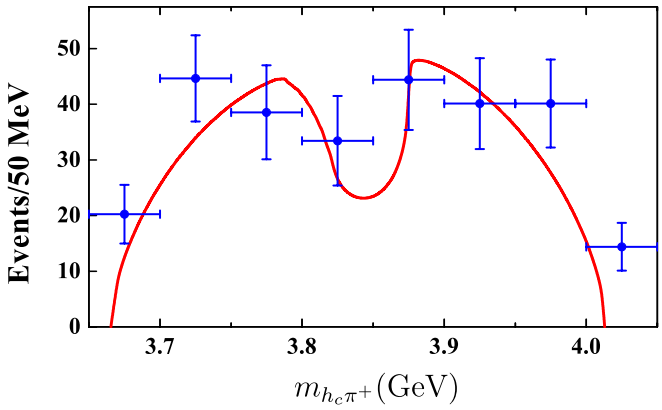


FIG. 6 (color online). (Color online.) A comparison of the $h_c\pi^\pm$ mass distribution of $\psi(4160) \to h_c(1P)\pi^+\pi^-$ (red solid line) predicted in this work and measurement by CLEO-c (blue points with errors) [31]. Here, CLEO-c measured the $h_c(1P)\pi^\pm$ mass distribution from $e^+e^- \to h_c(1P)\pi^+\pi^-$ at $E_{CM} = 4170$ MeV [31]. We normalize our numbers for a real comparison with the available CLEO-c data.

accumulating $\psi(4040)$ data with an aim to search for higher charmonia and the charmoniumlike states [30]. Our result shows the charged structures around the $D^*\bar{D}$ threshold in the $J/\psi\pi^+$, $\psi(2S)\pi^+$, and $h_b(1P)\pi^+$ invariant mass spectra of $\psi(4040)$ decays into $J/\psi\pi^+\pi^-$, $\psi(2S)\pi^+\pi^-$, and $h_b(1P)\pi^+\pi^-$, which are accessible at BESIII and could be considered in future studies.

Since these charged charmoniumlike structures also exist in the $J/\psi\pi^+$, $\psi(2S)\pi^+$, and $h_b(1P)\pi^+$ invariant mass spectra of $\psi(4260)$ hidden-charm dipion decays, carrying out the search for them will be an important and intriguing research topic, especially at Belle and *BABAR*.

If these predicted enhancement structures can be found in the higher charmonium and $Y(4260)$ hidden-charm decays, it will provide a direct test to the ISPE mechanism existing in the higher charmonium or $Y(4260)$ hidden-charm dipion decays.

## ACKNOWLEDGMENTS

X. L. would like to thank Chang-Zheng Yuan for suggestive discussions. This project is supported by the National Natural Science Foundation of China under Grant Nos. 10705001, No. 11005129, No. 11035006, No. 11047606, the Ministry of Education of China (FANEDD under Grant No. 200924, DPFIHE under Grant No. 20090211120029, NCET under Grant No. NCET-10-0442, the Fundamental Research Funds for the Central Universities), and the West Doctoral Project of Chinese Academy of Sciences.

*Note added.*—: after completion of this work, we noticed a measurement reported by CLEO-c [31]. Recently, the CLEO-c Collaboration announced the measurement of the $h_c(1P)\pi^\pm$ mass distribution from $e^+e^- \to h_c(1P)\pi^+\pi^-$ at $E_{CM} = 4170$ MeV (points with errors in Fig. 4 (b) of Ref. [31]). Thus, we compare the predicted $h_c\pi^\pm$ mass distribution of $\psi(4160) \to h_c(1P)\pi^+\pi^-$ (see Fig. 4) with the CLEO-c result. We notice that the predicted theoretical line shape of the $h_c(1P)\pi^\pm$ mass distribution of $\psi(4160) \to h_c(1P)\pi^+\pi^-$ in this work is consistent with the one measured by CLEO-c, which is listed in Fig. 6, where there indeed exists a broad structure around $D\bar{D}^*$ threshold and its reflection. To some extent, this fact provides a direct test to our prediction presented here.

[1] E. S. Swanson, Phys. Rep. **429**, 243 (2006).
[2] S. L. Zhu, Int. J. Mod. Phys. E **17**, 283 (2008).
[3] S. Godfrey and S. L. Olsen, Annu. Rev. Nucl. Part. Sci. **58**, 51 (2008).
[4] M. Nielsen, F. S. Navarra, and S. H. Lee, Phys. Rep. **497**, 41 (2010).
[5] N. Brambilla *et al.*, Eur. Phys. J. C **71**, 1534 (2011).
[6] I. Adachi *et al.* (Belle Collaboration), arXiv:1105.4583.
[7] Y. R. Liu, X. Liu, W. Z. Deng, and S. L. Zhu, Eur. Phys. J. C **56**, 63 (2008).
[8] X. Liu, Z. G. Luo, Y. R. Liu, and S. L. Zhu, Eur. Phys. J. C **61**, 411 (2009).
[9] A. E. Bondar, A. Garmash, A. I. Milstein, R. Mizuk, and M. B. Voloshin, arXiv:1105.4473.
[10] D. Y. Chen, X. Liu, and S. L. Zhu, arXiv:1105.5193.
[11] J. R. Zhang, M. Zhong, and M. Q. Huang, arXiv:1105.5472.
[12] Y. Yang, J. Ping, C. Deng, and H. S. Zong, arXiv:1105.5935.
[13] D. V. Bugg, arXiv:1105.5492.
[14] I. V. Danilkin, V. D. Orlovsky and Yu. A. Simonov, arXiv:1106.1552.
[15] T. Guo, L. Cao, M. Z. Zhou, and H. Chen, arXiv:1106.2284.
[16] Z. F. Sun, J. He, X. Liu, Z. G. Luo, and S. L. Zhu, arXiv:1106.2968.
[17] D. Y. Chen and X. Liu, arXiv:1106.3798.
[18] K. Nakamura *et al.* (Particle Data Group), J. Phys. G **37**, 075021 (2010).
[19] B. Aubert *et al.* (*BABAR* Collaboration), Phys. Rev. Lett. **95**, 142001 (2005).
[20] D. Y. Chen, J. He, and X. Liu, Phys. Rev. D **83**, 054021 (2011).
[21] Y. P. Kuang and T. M. Yan, Phys. Rev. D **24**, 2874 (1981).
[22] T. M. Yan, Phys. Rev. D **22**, 1652 (1980).
[23] V. A. Novikov and M. A. Shifman, Z. Phys. C **8**, 43 (1981).
[24] D. Y. Chen, J. He, X. Q. Li, and X. Liu, arXiv:1105.1672.
[25] Y. S. Oh, T. Song, and S. H. Lee, Phys. Rev. C **63**, 034901 (2001).
[26] R. Casalbuoni, A. Deandrea, N. Di Bartolomeo, R. Gatto, F. Feruglio, and G. Nardulli, Phys. Rep. **281**, 145 (1997).
[27] P. Colangelo, F. De Fazio, and T. N. Pham, Phys. Lett. B **542**, 71 (2002).
[28] A. Anastassov *et al.* (CLEO Collaboration), Phys. Rev. D **65**, 032003 (2002).
[29] C. Isola, M. Ladisa, G. Nardulli, and P. Santorelli, Phys. Rev. D **68**, 114001 (2003).
[30] http://english.ihep.cas.cn/prs/ns/201105/t20110511_69672.html.
[31] T. K. Pedlar *et al.* (CLEO Collaboration), arXiv:1104.2025.